Effect of Recent Revisions to the Geomagnetic Reversal Time-Scale On Estimates of Current Plate Motions

Article *in* Geophysical Research Letters · October 1994

DOI: 10.1029/94GL02118

CITATIONS
3,739

READS
1,904

4 authors:

C. Demets
University of Wisconsin–Madison
214 PUBLICATIONS **21,272** CITATIONS
SEE PROFILE

Richard G Gordon
Rice University
180 PUBLICATIONS **24,298** CITATIONS
SEE PROFILE

Donald F. Argus
NASA
109 PUBLICATIONS **19,053** CITATIONS
SEE PROFILE

Seth Stein
Northwestern University
221 PUBLICATIONS **23,018** CITATIONS
SEE PROFILE

EFFECT OF RECENT REVISIONS TO THE GEOMAGNETIC REVERSAL TIME SCALE ON ESTIMATES OF CURRENT PLATE MOTIONS

Charles DeMets [1], Richard G. Gordon[2], Donald F. Argus[3] ancl Seth Stein[2]

1) Department of Geology and Geophysics, University of Wisconsin, Madison
2) Department of Geological Sciences, Northwestern University, Evanston, Illinois
3) Jet Propulsion Laboratory, Cal Tech, Pasadena, California

Abstract. Recent revisions to the geomagnetic time scale indicate that global plate motion model NUVEL-1 should be modified for comparison with rates of motion estimated from space geodetic measurements. The optimal recalibration, which is a compromise among slightly different calibrations appropriate for slow, medium, and fast spreading rates, is to multiply NUVEL- 1 angular velocities by a multiplicative constant, α, of 0.9562. We refer to this simply recalibrated plate motion model as NUVEL- 1 A, and give correspondingly revised tables of angular velocities and uncertainties. Prior work has shown that space geodetic rates are slower on average than those calculated from NUVEL-1 by $6 \pm 1\%$. This average discrepancy is reduced to less than 2% when space geodetic rates are instead compared with NUVEL-1A.

Introduction

Global models of plate motions averaged over the past few million years are a useful standard for comparison with motions averaged over much shorter intervals, especially motions estimated from space geodetic measurements over approximately the past decade. In the past few years, the most widely used reference has been global plate motion model NUVEL- 1 [DeMets et al., 1990]. Recent revisions to the geomagnetic reversal time scale [Shackleton et al., 1990; Hilgen, 1991 ah], which are in better agreement with the observed spacing of marine magnetic anomalies across spreading centers [Wilson, 1993a; see also Gordon, 1993], suggest that the ages for geomagnetic reversals used in calibrating NUVEL-1 [i.e., those of Harland et al., 1982, which are the same as those of Mankinen and Dalrymple, 1979] are systematically too young. Therefore the angular speeds of plates in NUVEL-1 are systematically too fast. Herein we present and discuss a recalibration of NUVEL- 1 to remedy this systematic error by multiplying all NUVEL-1 angular velocities by a recalibration factor, α, of 0.9562, Tables describing this recalibrated model, which we refer to as NUVEL-1 A, are also presented.

The Effect of Time Scale Adjustments on Estimates of Spreading Rates

Aware that the time scale might eventually require adjustment, DeMets et al. [1990] previously sought to estimate spreading rates over as uniform a time interval as possible. If the time interval had been completely uniform and if the beginning of the time interval coincided with a magnetic reversal, revised spreading rates could now be found simply by multiplying the old rates by the ratio of the former to the current estimated age of the reversal. Herein we refer to this recalibration ratio as α.

The needed revision is not this simple, however. Magnetic anomalies corresponding to narrow polarity chrons can be resolved across fast-spreading centers, but not across slow-spreading centers, DeMets et al. [1990] fit the narrowest feature that could be resolved in the middle of the anomaly 2A sequence (which corresponds to the Gauss Normal Polarity Chron). Therefore the age of the feature fitted depended upon the spreading rate. For slow spreading rates ($\lesssim$ 25 mm/yr), they fit all of anomaly 2A because neither of the sub-chrons within chron 2A (i.e., the Kaena and Mammoth events) can be resolved in the anomaly (Figures 1 and 2). For intermediate spreading rates (between -25 and -55 mm/yr), the two reversed subchrons within chron 2A are manifested as a single, small negative anomaly within anomaly 2A (Figure 1), which is the feature that they fit. For fast spreading rates ($\gtrsim$ 55 mm/yr), the two reversed subchrons within chron 2A are manifested as distinct small negative anomalies; they fit the small positive anomaly between them.

Because the estimates of the ages of the reversals bounding each of these chrons or sub-chrons have been revised by different fractional amounts (Figure 2), the fractional revisions for slow, intermediate, and fast spreading differ slightly. Specifically, slow rates used in NUVEL-1 should be multiplied by a value for *a* of 0.9515, intermediate rates by 0.9529, and fast spreading rates by 0.9573. The uncertainties in these corrections are poorly known and these corrections may differ insignificantly.

To determine a single value for *a* by which one could multiply all spreading rates used in NUVEL-1, we sought the correction that minimizes the worst error in recalibration as measured in mm/yr. By a systematic search of values between 0.9529 and 0.9573, we found that the best factor to four significant figures is 0.9562. At the fastest "fast" rate of 160 mm/yr, this introduces a recalibration error of 0.18 mm/yr. At the fastest "intermediate" rate of 55 mm/yr, this introduces a recalibration error of –O. 18 mm/yr. The recalibration error at slow rates is less than 0.18 mm/yr if we use an age of 2.60 Ma as estimated by Shackleton et al. [1990] and adopted by Hilgen [1991 b] for the

young end of chron 2A.

With this particular recalibration, we have determined a new set of angular velocities by multiplying the old angular velocities by 0.9562 (Tables 1–3). We refer to this re-calibrated set of angular velocities (i.e., those multiplied by α = 0.9562) as NUVEL-1 A. Uncertainties were similarly re-calibrated. The uncertainties in rates of rotation are simply multiplied by α, while the uncertainties in the lengths of the major and minor axes of confidence ellipses are unchanged (Tables 1–3). Elements of the covariance matrix are revised by multiplication by α^2. in addition to the angular velocities determined by DeMets et al. [1990], we give in Table 1 the recalibrated angular velocities of the Juan de Fuca plate [Wilson, 1988, 1993b] and of the Philippine plate [Seno et al., 1987, 1993]. We have also added recalibrated angular velocities of the Rivera plate [DeMets and Stein, 1990] and of the Scotia plate [Pelayo and Wiens, 1989].

The recalibration has the unfortunate consequence of producing a new set of angular velocities that in nearly every case differ significantly from from those of NUVEL- 1. This is because NUVEL-1, like all previous global plate motion models, neglects the uncertainty in rates induced by uncertainties in the geomagnetic reversal time scale. These uncertainties have been neglected not so much because they are small—-although we must admit that the recent recalibration have been surprisingly large, but because the true size of the uncertainties are poorly known. This remains true today, Hilgen [1991 b] has suggested that the uncertainties are 1,000 to 2,000 years, but the results of Wilson [1993a] indicate that errors may be as large as 15,000 to 20,000 years. If Wilson's estimates are correct, then the additional uncertainties entirely attributable to time-scale uncertainties are about 0.5–0.7% of any rate. For applications for which time scale errors matter, especially for comparisons with geodetic rates, it is probably appropriate to add additional uncertainty of about this size.

Implications for the Steadiness of Plate Motion

Robbins et al. [1993] have compared rates of plate motion measured from satellite-laser ranging (SLR) and very long-baseline interferometry (VLBI) with those from NUVEL- 1. The correlation coefficient between SLR and VLBI data on the one hand and NUVEL-1 on the other is 0.994, but the space geodetic rates are on average slower by 6±1 %. Given that angular velocities in NUVEL-1 A are 4.4% slower than those in NUVEL- 1, this discrepancy shrinks to less than 2%. Therefore, the combined results from precise estimates of seafloor spreading, the revised geomagnetic reversal time scale, and space geodesy indicate that globally averaged plate motions are very steady, within a few per cent, over a time scale that ranges from several years to several million years [Argus and Gordon, 1990;

Ward, 1990; Smith et al., 1990; Robbins et al., 1993; Wilson, 1993a; Gordon, 1993]. Nonetheless for individual plate pairs, significant differences between the angular velocity averaged over the past few million years and that over the past few years are emerging. In particular, Argus and Gordon [1994] find an angular velocity of the Pacific relative to the North American plate averaged over the past -10 years that differs significantly from that presented here, mainly corresponding to a geologically recent speed up of Pacific-North American motion of 5±4 mm/yr (95% confidence limits) at a reference point in the Gulf of California.

Acknowledgements. We thank Bernard Minster and Mike Bevis for helpful comments. This work was begun while RGG was a visiting scientist at the Laboratoire de Geódynamique Sous-Marine and has been partially supported by NASA grant NAGS-885.

References

Argus, D. F., and R. G. Gordon, Pacific-North American plate motion from very long baseline interferometry compared with motion inferred from magnetic anomalies, transform faults, and earthquake slip vectors, *J. Geophys. Res.*, 95, 17,315-17,324, 1990.

Argus, D. F., and R. G. Gordon, No-net-rotation model of current plate velocities incorporating plate motion model NUVEL-1, *Geophys. Res. Lett.*, 18, 2038-2042, 1991.

Argus, D. F., and R. G. Gordon, Horizontal surface velocities estimated from VLBI: Plate motion and crustal deformation, *Geophys. J. Int.*, to be submitted, 1994.

DeMets, C., R. G. Gordon, D. F. Argus, and S. Stein, Current plate motions, *Geophys. J. Int.*, *101*, 425-478, 1990.

DeMets, C., and S. Stein, Present-day kinematics of the Rivera plate and implications for tectonics of southwestern Mexico, *J. Geophys. Res.*, 95, 21,931-21,948, 1990.

Gordon, R. G., Orbital dates and steady rates, *Nature*, 364, 760–761, 1993.

Harland, W. B., A. V. Cox, P. G. Llewellyn, C. A. G. Pickton, A. G. Smith, and R. Walters, *A Geologic Time Scale*, 131 pp., Cambridge Univ. Press, New York, 1982.

Hilgen, F. J., Astronomical calibration of Gauss to Matuyama sapropels in the Mediterranean and implications for the geomagnetic polarity time scale, *Earth Planer. Sci. Lett.*, 104, 226-244, 1991 a.

Hilgen, F. J., Extension of the astronomically calibrated (polarity) time scale to the Miocene/Pliocene boundary, *Earth Planet. Sci. Lett.*, 107, 349-368, 1991 b.

Mankinen, E. A., and G. B. Dalrymple, Revised geomagnetic

polarity time-scale for the interval O--5 my. BP, *J. Geophys. Res., 84, 615-626,* 1 *979.*

Pelayo, A. M., and D.A. Wiens, Seismotectonics and relative plate motions in the Scotia Sea region, *J. Geophys. Res., 94, 7293-7320,* 1989.

Robbins, J. W., D.E. Smith, and C. Ma, Horizontal crustal deformation and large scale plate motions inferred from space geodetic techniques, in *Contributions of Space Geodesy to Geodynamics: Crustal Dynamics, Geodynamic Series* 23, edited by D. E. Smith and D. L. Turcotte, pp. 21 –36, American Geophysical Union, Washington, 1993.

Seno, T., T. Moriyama, S. Stein, D.F. Woods, C. DeMets, D. Argus, and R. Gordon, Redetermination of the Philippine sea plate motion (abstract), *Eos Trans.* AGU, 68, 1474, 1987.

Seno, T., S. Stein, and A. E. Gripp, A model for the motion of the Philippine sea plate consistent with NUVEL-1 and geological data, *J. Geophys. Res.,* 98, 17,941–1 7,948, 1993.

Shackleton, N. J., A. Berger, and W. R. Peltier, An alternative astronomical calibration of the lower Pleistocene timescale based on ODP Site 677, *Transactions of the Royal Society of Edinburgh: Earth Sciences, 81, 251 –261,* 1990.

Smith, D. E., R. Kolenkiewicz, P. J. Dunn, J. W. Robbins, M. H. Torrence, S. M. Klosko, R. G. Williamson, E. C. Pavlis, N. B. Douglas, and S. K. Fricke, Tectonic motion and deformation from satellite laser ranging to LAGEOS, *J. Geophys. Res.,* 95, 22,013--22,041, 1990.

Ward, S. N., Pacific-North America plate motions: New results from very long baseline interferometry, *J. Geophys. Res.,* 95, 21 ,965–21 ,981, 1990.

Wilson, D.S., Confirmation of the astronomical calibration of the magnetic polarity timescale from sea-floor spreading rates, *Nature, .?64, 788–790,* 1993a.

Wilson, D. S., Confidence intervals for motion and deformation of the Juan de Fuca plate, *J. Geophys. Res.,* 98, 16,053-16,071, 1993b.

Fig. 1, Observed marine magnetic anomaly profiles across fast, intermediate, and slow spreading centers are compared with synthetic profiles, As can be seen in both the observed and synthetic profiles, brief subchrons are better resolved within anomaly 2A as spreading rate increases. The profile across a slow spreading center (Africa-North America) shows only a single positive anomaly for chron 2A with a slight inflection that may be caused by crust magnetized during the Kaena and Mammoth reversed polarity subchrons (cf. Fig. 2). The profile across an intermediate-rate spreading center (Central Indian Ridge) shows two positive anomalies flanking a negative anomaly in the anomaly 2A sequence. The negative anomaly resolves the combined Kaena and Mammoth polarity subchrons, but not the brief normal polarity interval between them. The profile across a fast spreading center (Southeast Indian Ridge) shows two distinct negative anomalies, corresponding to distinct Kaena and Mammoth reversed subchrons, separated by a narrow positive anomaly corresponding to the brief normal polarity interval between them.

Fig. 2. Comparison of time scale used herein (i.e., that of Hilgen [1991 b], which incorporates that of Shackleton et al. [1990] for 0-2.60 Ma) with the time scale of Harland et al. [1982] used in deriving NUVEL-1. The tilled circles in the recalibration diagram shown at right show the ratio of the age of a reversal adopted by Harland et al. [1982] to that adopted by Hilgen [1991 b]. Note that the recalibration factors for the Gauss normal polarity chron, corresponding to anomaly 2A, which is the reference anomaly in NUVEL-1, are nearer one and therefore require less revision than those for the Brunhes, Matuyama, and Gilbert polarity chrons. The vertical line labeled "A" shows the best recalibration for profiles across slow spreading centers, the vertical line labeled "B" shows the best recalibration for profiles across intermediate spreading centers, and the vertical line labeled "C" shows the best recalibration for profiles across fast spreading centers. The difference (0.0058) between recalibration "A" and recalibration "C" is eight times smaller than the difference between the old and new time scales. The vertical line labeled "O" shows the optimal recalibration, which minimizes the worst error in calibration across all spreading rates and is adopted in this paper.

Table 1. NUVEL-1A Angular Velocities (Pacific Plate Fixed)

Plate	Latitude °N	Longitude °E	ω (deg–m.y.$^{-1}$)	ω_x	ω_y (radians–m.y.$^{-1}$)	ω_z
Africa	59.160	-73.174	0.9270	0.00240 I	-0.007939	0,013892
Antarctica	64.315	-83.984	0.8695	0.000689	-0,006541	0.013676
Arabia	59.658	–33.]93	1.1107	0.008195	--0,005361	0.016730
Australia	60.080	1.742	1.0744	0.009349	0.000284	0.016252
Caribbean	54.195	-80.802	0.8160	0.001332	-0.008225	0.011551
Cocos	36.823	-108.629	1.9975	-0.008915	-0.026445	0.020895
Eurasia	61.066	-85.819	0.8591	0.000529	-0.007235	0.013123
India	60.494	-30,403	I.1034	0.008180	-0.004800	0.016760
Nazca	55.578	-90.096	1.3599	-0.000022	-0.013417	0.019579
North America	48.709	-78.167	0.7486	0.001768	-0.008439	0.009817
South America	54.999	-85.752	0.6365	0.000472	-0.006355	0.009100
Additional Angular Velocities (Pacific Plate Fixed)						
Juan de Fuca[1]	35.0	26.0	0.51	0.00651	0.00317	0.00508
Juan de Fuca[2]	28.3	29.3	0.519	0.00670	0.00376	0,00414
Philippine[3]	o.	-47,	0.96	0.0114	-0.0122	0.0000
Philippine	-1.2	-45.8	0.96	0.0116	-0.0120	0.0003
Rivera[5]	31.0	-102.4	2.45	-0.00788	-0.03580	0.02202
Scotia[6]	49.1	-81.4	0.66	0.0011	-0.0075	0.0087
NNR Ref. Frame[7]	63.0	-72.6	0,6411	–0.00151	0.00484	-0.00997

Each named plate moves counterclockwise relative to the Pacific plate. Footnotes: 1) Recalibrated from Wilson [1988]; this angular velocity was incorporated into model NNR-NUVEL1. 2) Recalibrated from the more recent estimate of Wilson [1993]. 3) Recalibrated from Seno *et al.* [1987]; this angular velocity was incorporated into model NNR-NUVEL1 [Argus and Gordon, 1991]. 4) Recalibrated from the more recent estimate of Seno *et al.* [1993]. 5) Recalibrated from DeMets and Stein [1990], 6) Derived from Scotia plate velocity model described in Pelayo and Wiens [1989]. Depends in part on spreading rates averaged over -1.9 Ma (Anomaly 2), shorter than the 3.1 -million year averaging interval used in NUVEL-1A. 7) Angular velocity of no-net-rotation reference frame relative to the Pacific plate, recalibrated from Argus and Gordon [1991].

Table 2a. NUVEL-1A Angular Velocities:
Pairs of Plates Sharing a Boundary

Plate Pair	Latitude °N	Longitude °E	ω (deg–m.y.$^{-1}$)	Error Ellipse σ_{max}	σ_{min}	ζ_{max}	σ_ω (deg–m.y.$^{-1}$)
			Pacific Ocean				
na-pa	48.7	-78.2	0.75	1.3	1.2	-61	0.01
ri-pa	31.0	-102.4	2,45	3.6	0.6	21	0.57
co-pa	36.8	-108.6	2.00	1.0	0.6	-33	0.05
ri-na	22.8	-109.4	1.80	1.8	0.6	-S7	0.58
ri-co	6.8	-83.7	0.54	38.3	1.8	-56	0.52
co-na	27.9	-120.7	1.36	1.8	0.7	-67	0.05
CO-117.	4,8	–124.3	0.91	2.9	1.5	-88	0.05
n 7.-pa	55.6	-90.1	1.36	1.8	0.9	-1	0.02
nz-an	40.5	-95.9	0.52	4.5	1.9	-9	0.02
nz-sa	56.0	-94.0	0.72	3.6	1.5	–10	0.02
an-pa	64.3	-84.0	0.87	1.2	1.0	81	0.01
pa-au	-60.1	–178.3	1.07	1.0	0.9	-58	0.01
eu-pa	61.1	-85.8	0.86	1.3	1.1	90	0.02
co-ca	24.1	-119.4	1.31	2.5	1.2	-60	0.05
nz-ca	S6.2	-104.6	0.55	6.5	2.2	–31	0.03
			A tlantic Ocean				
eu-na	62.4	135.8	0.21	4.1	1.3	–11	0.01
af-na	78.8	38.3	0.24	3,7	1.0	77	0.01
af-eu	21.0	-20.6	0.12	6.0	0.7	-4	0.02
na-sa	16.3	–58.1	0.15	5.9	3.7	–9	0.01
áf-sa	62.5	-39.4	0.31	2.6	0.8	–11	0.01
an-sa	86.4	-40.7	0.26	3.0	1.2	–24	0.01
na-ca	-74.3	-26.1	0.10	25.5	2.6	-52	0.03
ca-sa	50.0	-65.3	0.18	15.1	4.3.	-2	0.03
			Indian Ocean				
au-an	13.2	38,2	0.65	1.3	1.0	-63	0.01
af-an	5.6	-39.2	0.13	4.4	1.3	-42	0.01
au-af	12.4	49.8	0.63	1.2	0.9	-39	0.01
au-in	-5.6	77.1	0,30	7.4	3.1	-43	0.07
in-af	23.6	28.5	0.41	8.8	1.5	-74	0.06
ar-af	24.1	24.0	0.40	4.9	1.3	-65	0.05
in-eu	24.4	17.7	0.51	8.8	1.8	-79	0.05
ar-eu	24.6	13.7	0.50	5.2	1.7	-72	0.05
au-eu	15.1	40.5	0.69	2.1	1.1	-45	0.01
in-ar	3.0	91.5	0.03	26.1	2.4	-58	0.04

The first plate moves counterclockwise relative to the second plate. Plate abbreviations: pa, Pacific; na, North America; sa, South America; af, Africa; co, Cocos; nz, Nazca; eu, Eurasia; an, Antarctica; ar, Arabia; in, India; au, Australia; ca, Caribbean. See Figure 3 for plate geometries, One sigma-error ellipses are specified by the angular lengths of the principal axes and by the azimuths (ζ_{max}, given in degrees clockwise

from north) of the major axis. The rotation rate uncertainty is determined from a one-dimensional marginal distribution, whereas the lengths of the principal axes are determined from a two-dimensional marginal distribution.

Table 2b. NUVEL - 1A Angular Velocities:
Pairs of Plates not Sharing a Boundary

Plate Pair	Latitude °N	longitude °E	ω (deg–m.y.$^{-1}$)	Error Ellipse σ_{max}	σ_{min}	ζ_{max}	σ_ω (deg–m.y.$^{-1}$)
ca-af	-64.7	-165.0	0.15	19.5	9.8	-86	0.02
co-at"	17.9	-121.4	1.31	1.7	0.8	-83	0.05
nz-af	43.5	-113'.9	0.47	5.2	2.2	–26	0.02
ar-an	21.9	8.9	0.47	5.9	1.6	-80	0.04
ca-an	-49.7	-69.1	0.16	17.3	5.1	-06	0.03
co-an	18.1	-115.8	1.33	1.4	0.8	-78	0.05
eu-an	-37.8	-103.0	0.05	25.1	14.5	49	0.01
in-an	21.9	13.1	0.47	9.9	1.7	-84	0.05
ar-au	4.7	–101.6	0.33	7.5	2.4	61	0.05
ar-ca	34.9	22.7	0.52	7.0	4.6	-63	0,05
au-ca	21.9	46.7	0.72	3.9	3,2	–56	0.02
in-ca	34.2	26.6	0.53	9.4	4.4	-66	0.06
ar-co	-8.7	50.9	1.57	1.8	1.2	-72	0.07
au-co	-8.2	55.7	1.87	1.3	0.6	-79	0.05
in-co	–8.5	51.7	1.60	1.9	1.3	73	0.08
ca-eu	-51.0	-50.9	0.12	22.7	6.5	-25	0.03
co-eu	20.0	-116.2	1.30	1.6	1.0	–81	0.05
nz-eu	46.1	-95.1	0.51	4.8	2.S	-09	0,02
an-na	60.5	119.6	0.24	4.2	2.0	-22	0.01
ar-na	44.1	25.6	0.57	4.8	1.4	-39	0.04
au-na	29.1	49.0	0.76	1.6	1.0	-53	0,01
in-na	43.3	29.6	0.58	7.5	1.5	-52	0.05
nz-na	61.5	-109.8	0.64	4.0	1.8	-24	0.02
ar-nz	-13.9	44.4	0.68	4.2	2.2	31	0.05
au-nz	–11.3	55.6	0.97	2.2	1.3	43	0.02
in-nz	–13.3	46.4	0.70	5.3	1.9	42	0.07
af-pa	59.2	-73.2	0.93	1.1	1.0	86	0.01
ar-pa	59.7	–33.2	1.11	3.8	0.9	-88	0.02
ca-pa	54.2	-80.8	0.82	3.4	1.2	–11	0.03
in-pa	60.5	-30.4	1.10	5.5	1.1	82	0.02
sa-pa	55.0	-85.8	0.64	1.8	1.6	-64	0.01
af-ri	–15.3	69.7	1.76	3.1	1.0	-33	0.58
an-ri	–15.3	73.7	1.81	2.6	0.9	04	0.58
ar-ri	-8.7	62.2	2.00	6.7	0.9	41	0.56
au-ri	-8 2	64.5	2.32	5.4	0,8	-34	0.56
ca-ri	-19.8	61.5	1.77	1.6	1.3	59	0.58
eu-ri	-16.6	73.6	1.78	2.1	1.0	04	0.58
in-ri	-8.6	62.6	2.02	6.5	1.1	-39	0.56
nz-ri	–5.9	70.7	1.37	9.0	1.5	-lo	0.56
sa-ri	-22.9	74.2	1.90	1.1	1.0	--10	0.58
ar-sa	44,4	7.3	0.62	5.2	1.5	-59	0.04
au-sa	32.8	36.8	0.76	1.3	1.2	18	0.01
co-sa	28.0	-115.0	1.44	1.5	0.8	-56	0.05
eu-sa	77.6	-86.3	0.24	4.8	1.4	-66	0.02
in-sa	44.2	11.4	0.63	8.1	1.7	-69	0.04

The conventions are the same as in Table 2a.

Table 3. Best-fitting and Closure-fitting Angular Velocities

Plate Pair	Best-fitting Lat. °N	Long. °E	ω (deg–m.y.$^{-1}$)	Error Ellipse σ_{max}	σ_{min}	ζ_{max}	σ_ω (deg–m.y.$^{-1}$)	Closure-fitting Lat. °N	Long. °E	ω (deg–m.y.$^{-1}$)
				Pacific Ocean						
na-pa	*49.6*	*–76.7*	0.71	3.1	1.5	66	0.04	48.3	-77.0	0,76
ri-pa	31.0	*-77.6*	2.45	3.6	0.6	21	0.54	--------		----
co-pa	*34.4*	*–108.6*	2,20	1.6	0.8	-12	0.10	37.3	-108,7	1.96
co-nz	5.2	*-125.8*	0.87	4.1	1.8	-88	0.06	4.9	-121.6	1.12
nz-pa	*53.8*	*--88.2*	1.36	8.2	2.6	19	0.03	55.8	-90.4	1.36
nz-an	*35.0*	*-97.9*	0.54	20.1	2.8	-2	0.04	40.3	–93.9	0.51
nz-sa	*74.7*	*–106.3*	----	62.1	2.1	–30	----	53.2	–97.5	0.73
an-pa	65.1	-80.6	0.88	2.3	1.6	34	0.02	64.6	-85.8	0.86
na-co	1.0	-73.2	----	107,5	1.8	-56	----	28.3	-120.3	1.36
ca-co	7.2	-79.9	----	3.3	0.4	--65	----	22.2	-119.2	1.29
				Atlantic Ocean						
eu-na	63.2	134.5	0.22	*4.8*	*1.4*	*-12*	0.01	61.3	139.3	0.21
af-eu	22.7	–20.7	----	7.0	0.7	-04	----	19.5	-23.7	0.13
af-na	73.7	94.8	0.21	14.7	1.4	-40	0.01	74.3	17.2	0.26
af-sa	63.4	–39.4	0.31	3.0	0.8	–11	0.01	66.9	–43.8	0.35
an-sa	86.0	-40.5	0.29	8.9	1.4	-25	0.05	88.7	–36.1	0.26
ca-na	30.2	108.6	0.17	20.9	2.1	13	0.07	--------		----
ca-sa	70.3	–167.9	----	1193	10	79	----	63.1	–15.2	0.12
				Indian Ocean						
in-af	*25.5*	*26.8*	039	*16.5*	*2.8*	*--67*	0.10	23.4	26.9	0.39
ar-af	23.8	23.4	0,39	*6.2*	*1.6*	*-68*	0.06	24.7	-18,8	0.39
au-af	1.7	50,8	0.65	*6.2*	*1.0*	*-34*	0.07	11.1	49,0	0.63
au-an	12.1	37.7	0.65	*1.7*	*1.6*	*–38*	0.01	12.7	39.8	0.67
af-an	6.()	–39.3	0.14	*6.7*	*1.4*	*-45*	0.01	-1.8	-40.4	0.12
in-ar	0.8	95.0	----	33.1	2.7	–58	----	27.9	123.0	0.02

First plate moves counterclockwise relative to second plate. Plate abbreviations: pa, Pacific; na, North America; sa, South America; af, Africa; co, Cocos; nz, Nazca; eu, Eurasia; an, Antarctica; ar, Arabia; in, India; au, Australia; ca, Caribbean. One sigma-error ellipses are specified by the angular lengths of the principal axes and by the azimuths (ζ_{max}, given in degrees clockwise from north) of the major axis. The rotation rate uncertainty is determined from a one-dimensional marginal distribution, whereas the lengths of the principal axes are determined from a two-dimensional marginal distribution.

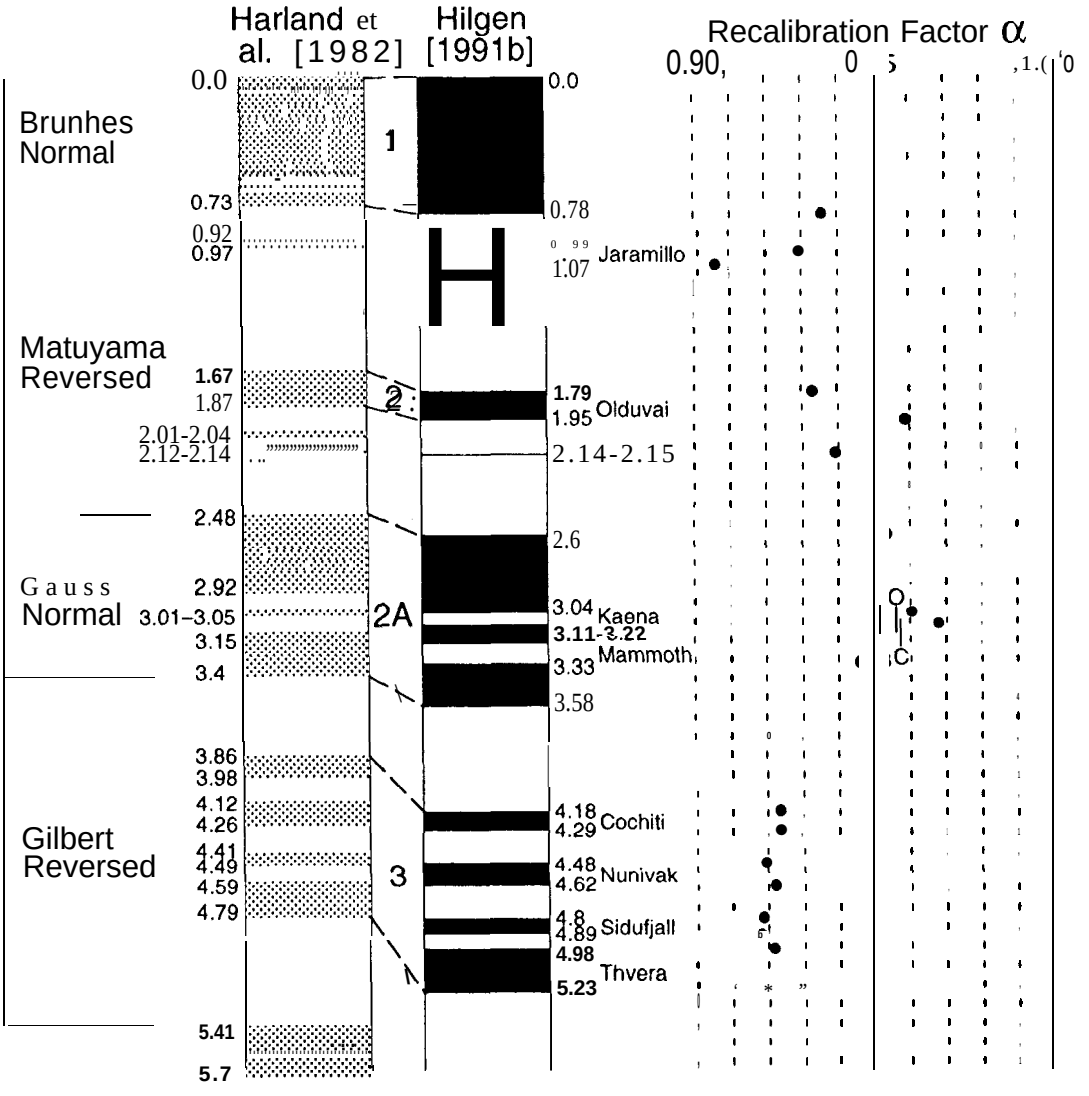
Harland et al. [1982]
Hilgen [1991b]
Recalibration Factor α
Brunhes Normal
Matuyama Reversed
Gauss Normal
Gilbert Reversed
0.0
0.73
0.92
0.97
1.67
1.87
2.01-2.04
2.12-2.14
2.48
2.92
3.01–3.05
3.15
3.4
3.86
3.98
4.12
4.26
4.41
4.49
4.59
4.79
5.41
5.7
1
2
2A
3
0.78
1.07
Jaramillo
1.79
1.95
Olduvai
2.14-2.15
2.6
3.04
Kaena
3.11-3.22
Mammoth
3.33
3.58
4.18
4.29
Cochiti
4.48
4.62
Nunivak
4.8
4.89
Sidufjall
4.98
5.23
Thvera

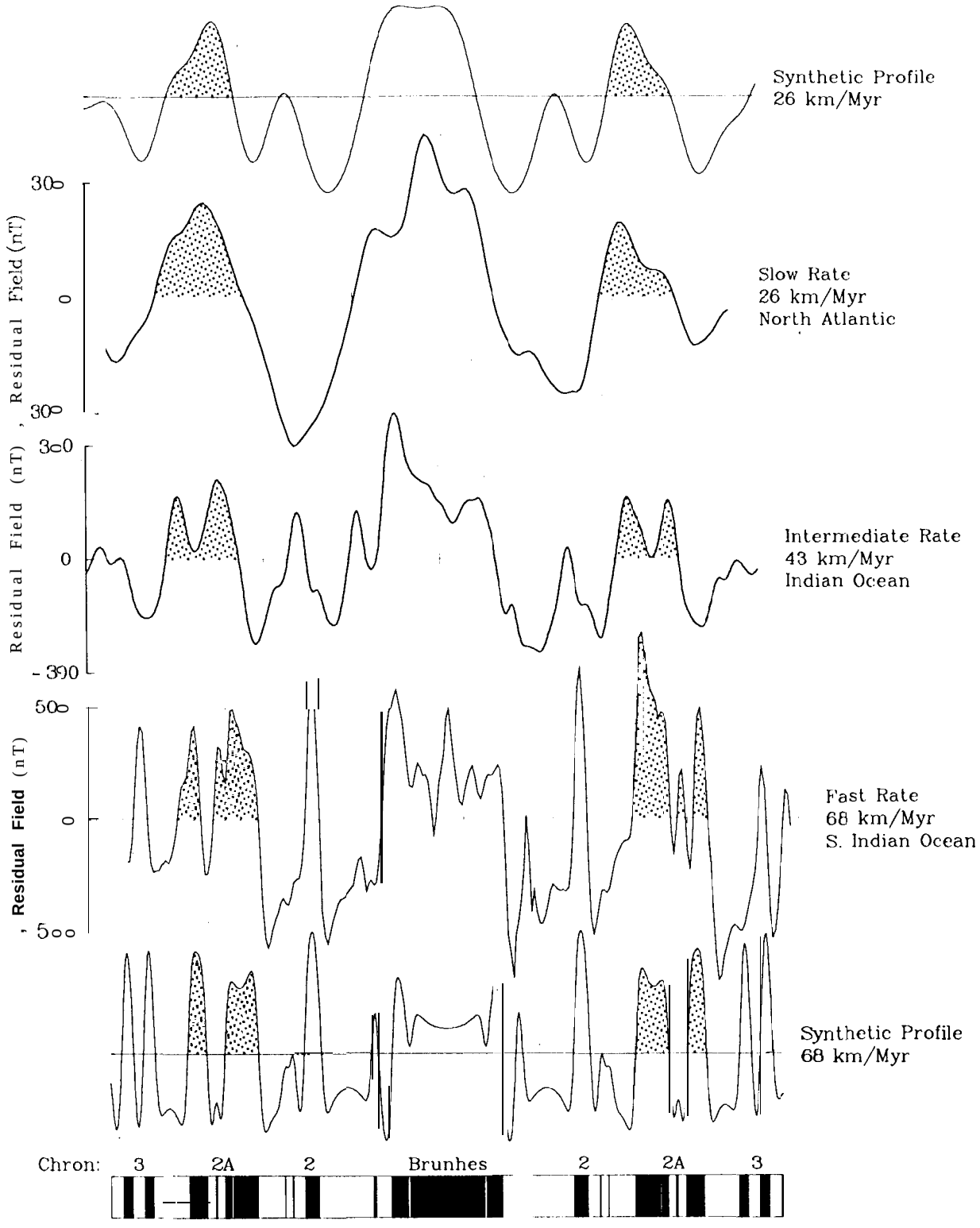
Synthetic Profile
26 km/Myr
Slow Rate
26 km/Myr
North Atlantic
Intermediate Rate
43 km/Myr
Indian Ocean
Fast Rate
68 km/Myr
S. Indian Ocean
Synthetic Profile
68 km/Myr
Residual Field (nT)
300
0
-300
500
0
-500
Chron:
3
2A
2
Brunhes
2
2A
3